Supramolecular Chemistry
Publication details, including instructions for authors and subscription information:
http://www.informaworld.com/smpp/title~content=t713649759

Self-assembly of Au Nanoparticle-containing Peptide Nano-rings on Surfaces

Nurxat Nuraje[a]; Kai Su[b]; Jacopo Samson[a]; Amit Haboosheh[a]; Robert I. Maccuspie[a]; Hiroshi Matsui[a]
[a] Department of Chemistry, Hunter College and the Graduate Center, City University of New York, New York, NY, USA [b] Department of Chemistry, College of Staten Island, Staten Island, NY, USA

To cite this Article Nuraje, Nurxat , Su, Kai , Samson, Jacopo , Haboosheh, Amit , Maccuspie, Robert I. and Matsui, Hiroshi(2006) 'Self-assembly of Au Nanoparticle-containing Peptide Nano-rings on Surfaces', Supramolecular Chemistry, 18: 5, 429 — 434
To link to this Article: DOI: 10.1080/10615800600659196
URL: http://dx.doi.org/10.1080/10615800600659196

Supramolecular Chemistry, July–August 2006 Vol. 18 (5), pp. 429–434

Taylor & Francis
Taylor & Francis Group

Self-assembly of Au Nanoparticle-containing Peptide Nano-rings on Surfaces

NURXAT NURAJE[a], KAI SU[b], JACOPO SAMSON[a], AMIT HABOOSHEH[a], ROBERT I. MACCUSPIE[a] and HIROSHI MATSUI[a,*]

[a]*Department of Chemistry, Hunter College and the Graduate Center, City University of New York, New York, NY 10021, USA;* [b]*Department of Chemistry, College of Staten Island, Staten Island, NY 10314, USA*

(Received 5 December 2005; Accepted 16 February 2006)

The peptide nano-rings containing Au nanoparticles inside their cavities were self-assembled on dithiol SAMs patterned as an array by AFM-based nanolithography. The peptide nano-rings were aligned as a line on these SAMs, and Au formed lines with the spacing between these nanoparticles as the peptide nano-rings functioned as spacers. This type of array fabrication will provide improved tunability in their optical properties of resulting nanoparticle-assembled arrays. In addition, optimization of the inter-particle distance of nanoparticles in the array with various spacers may allow one to design new types of photonic crystals with desired optical properties.

Keywords: Peptide nano-rings; Bionanotechnology; Nanofabrication; Self-assembled monolayers

INTRODUCTION

Recent improved two-dimensional and three-dimensional nanofabrication techniques allow one to build precisely designed structures in nanoscale for various photonic applications [1–3]. While the top–down approach has been applied for photonic crystal fabrications, the bottom–up approach via self-assembly of photonic nano-building blocks is also showing promising outcomes [4–12]. For the bottom–up approach for the optics fabrications, synthesis of photonic nanomaterials and their alignments need to be accomplished efficiently and precisely.

Biomineralization process, where peptides or proteins are utilized to mineralize metals and semiconductors, has been shown to produce various types of nanocrystals [13–25]. Since the amino acid sequences are very sensitive to elements for their mineralization, optimized peptide sequences can produce nanocrystals efficiently [26]. In addition to the effective crystal growth, the amino acid sequences of mineralizing peptides could also influence the size, the alignment, and the shape of resulting nanocrystals [27–30]. Further more, in some cases, peptides could mineralize nanocrystals in solution at room temperature that do not grow under the ambient condition [31,32]. Because the size, the alignment, the shape, and the crystalline structure of photonic nanocrystals control optical properties of those assembled nanocrystals, the tunabilities of these features and the potential of new material synthesis by using peptides will provide a significant advantage to apply peptides for photonic material syntheses.

The one of smart approaches to create photonic materials by using mineralizing peptides is to pattern these peptides on surfaces based on photonic device designs and grow photonic crystals on the patterned peptides. For example, a hologram was applied to pattern silica-mineralizing peptides as an array and resulting silica nanostructures exhibited a nearly fifty-fold increase in diffraction efficiency over a comparable polymer hologram [14]. Recently, microfluidics and lithography were also used to pattern silica- and silver-mineralizing peptides for photonic applications [28,33].

In this report, we assembled ring-shaped peptide nanostructures as an array on surfaces. Previously, we developed the ring-shaped peptide nanostructures by self-assembling a peptide monomer, bis(*N*-α-amidoglycylglycine)-1,7-heptane dicarboxylate and an organic

*Corresponding author. E-mail: hmatsui@hunter.cuny.edu

ISSN 1061-0278 print/ISSN 1029-0478 online © 2006 Taylor & Francis
DOI: 10.1080/10615800600659196

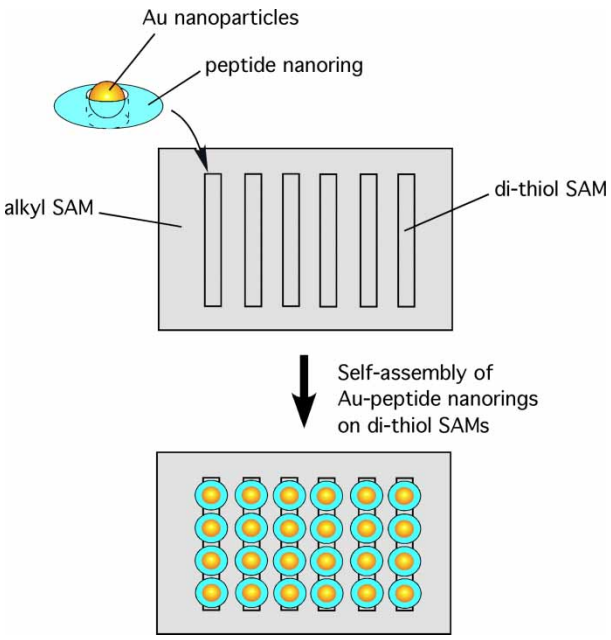

FIGURE 1 Illustration of Au nanoparticle-containing peptide nano-ring assembly on the patterned Au substrate.

Au precursor, trimethylphosphinegold chloride ($AuPMe_3Cl$) in solution [34]. After reduction of Au ions trapped inside the cavities of nano-rings, the peptide nano-rings could template Au nanoparticles. In this report, after Au nanoparticles were grown inside the cavities of the peptide nano-rings, these nano-rings containing Au nanoparticles were aligned on the chemically functionalized arrays patterned by nano-lithography (Fig. 1). Since these peptide nano-rings were self-assembled in a closely packed manner along the array of those dithiolated self-assembled monolayers (SAMs), these Au nanoparticles were positioned in the equal spacing on each line without touching each other as the peptide nano-rings functioned as spacers. This type of alignment of nanomaterials with spacers can be very useful for improved photonic crystal designs.

RESULTS AND DISCUSSION

When the peptide monomers were self-assembled in the presence of the water-insoluble trimethylphosphinegold chloride ($AuPMe_3Cl$) for 5 days in the dark, the ring-shaped peptide assemblies were observed in solution. The average outer diameter of nano-ring was 50 nm and the average inner diameter was 15 nm [34]. Our previous spectroscopic investigation showed that these peptide nano-rings were self-assembled from the peptide monomers and the organic Au salts by chelating Au with amide groups of the peptide monomers. After UV light was irradiated to the nano-ring solution for 20 min Au nanoparticles were grown inside the cavities of nano-rings, however the organic Au salts, trapped inside the cavities, were reduced to grow Au nanoparticles in the middle of nano-rings [34,35]. In a TEM image of the nano-ring after reduction of Au ions, the Au nanoparticle appeared darker at the center of the nano-ring (Fig. 2a). These particles in the cavities were also confirmed as Au nanoparticles by electron diffraction before their surface assembly on the dithiol SAMs.

When the peptide nano-rings were previously synthesized, they were observed to be stable in solution [34] however these nano-rings have not been assembled on surfaces. Therefore, it was necessary to examine their stability via the simple surface-assembly. Before fabricating the structure shown in Fig. 1, we examined whether the Au nanoparticle-containing peptide nano-rings are rigid enough to be self-assembled on surfaces by spin-coating them on TEM grids. A height image of AFM

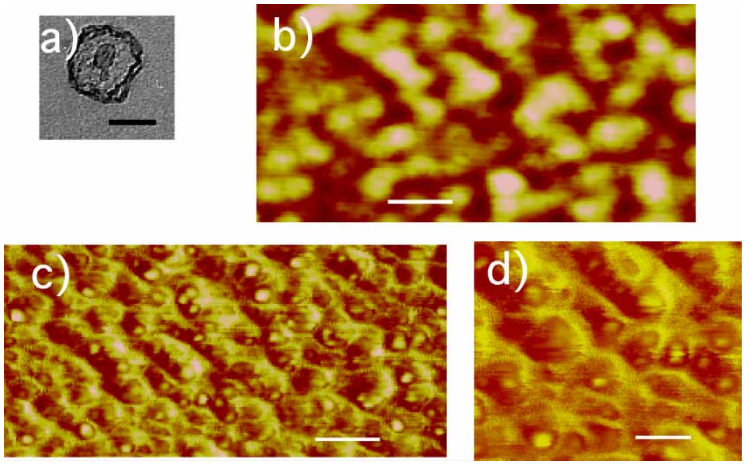

FIGURE 2 (a) TEM image of the peptide nano-ring containing a Au nanoparticle inside the cavity, scale bar = 50 nm. (b) AFM image of spin-coated peptide nano-rings containing Au nanoparticles in their cavities on TEM grids in height mode, scale bar = 80 nm (c) AFM image of spin-coated peptide nano-rings containing Au nanoparticles in their cavities on TEM grids in phase mode, scale bar = 80 nm (d) the phase AFM phase image in high magnification, scale bar = 40 nm.

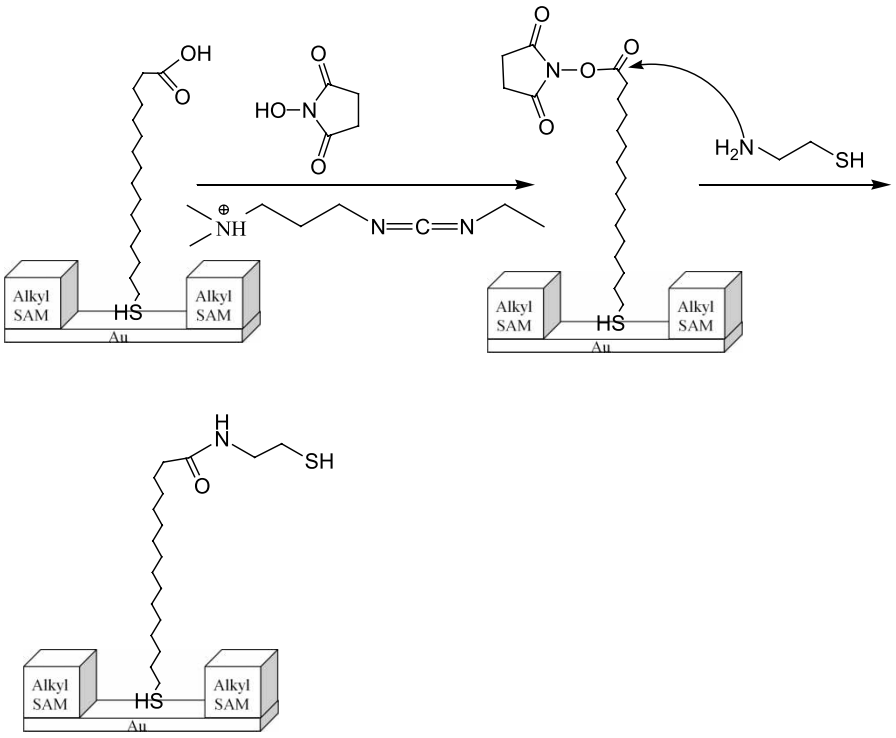

SCHEME 1 Fabrication of dithiol SAMs on patterned Au substrates.

in Fig. 2b confirms that the nano-rings were deposited on a TEM grid. This figure imaged the assembly of the nano-rings on the surface, but the Au nanoparticles inside the nano-rings could not be resolved in this AFM height image. However, when this assembly was imaged by the phase mode of AFM as shown in Fig. 2c, the Au nanoparticles were observed as a brighter contrast inside the nano-rings because harder surfaces of Au nanoparticles appeared brighter than softer surfaces of the outer peptide nano-rings. In the magnified phase image of Fig. 2d, these Au nanoparticles were not exactly located at the center of the nano-rings, which may be due to the deformation of the nano-ring shape via spin-coating and the multiple orientations of the nano-rings on TEM grids.

Since the peptide nano-rings were stable enough to be assembled on TEM grids via spin-coating, we examined the targeted self-assembly of the peptide nano-rings on the functionalized surfaces. The functionalized array of dithiol SAMs was patterned by three steps. First, alkyl SAMs were deposited on a Au substrate and the array was patterned by removing the alkyl SAMs with the AFM cantilever. Then, mercaptohexadecanoic acid was assembled on the curved array where Au surfaces were exposed. The carboxylic groups on the top of these SAMs on trenches were substituted by thiol groups, as shown in Scheme 1. To align the peptide nano-rings containing Au nanoparticles on the dithiol SAM array patterned on a Au substrate as shown in Fig. 1, these nano-rings were incubated with this substrate in solution for 8 h. Because the end groups of the SAMs on the trenches were functionalized by thiol (Scheme 1), this incubation process allowed the nano-rings to self-assemble onto these trenches with the thiol-Au interaction, as shown in Fig. 3. Figure 3a is the AFM image of the patterned substrate in the height mode after the nano-rings were incubated in the substrate-containing solution. The peptide nano-rings were closely packed to form the array of continuous lines along the trenches

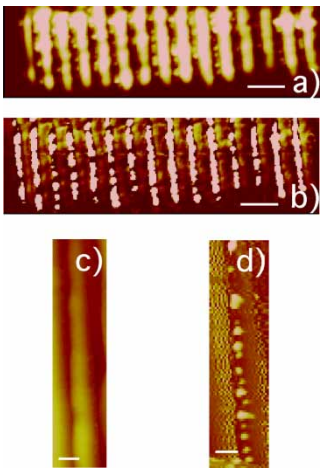

FIGURE 3 AFM images of Au nanoparticle-containing peptide nano-rings assembled on the dithiol SAM-patterned in (a) height mode, scale bar = 300 nm (b) phase mode, scale bar = 300 nm (c) height mode in high magnification, scale bar = 50 nm, (d) phase mode in high magnification, scale bar = 50 nm.

in Fig. 3a. As seen in the height mode AFM image of the spin-coated samples in Fig. 2b, the individual Au nanoparticle inside the nano-ring could not be identified in Fig. 3a due to their small height difference between the peptide nano-ring and the Au nanoparticle. However, when the phase mode of AFM was applied to image this substrate, the deposited spheres on the trenches looked less continuous in Fig. 3b since the brighter spheres in this phase image are more likely Au nanoparticles due to their surface hardness as compared to the one for the peptide nano-rings. While these AFM images in the phase mode in low resolution do not explicitly show the discrete positioning of Au nanoparticles inside the nano-rings aligned on the trenches as shown in Fig. 1, the high-resolution image of the single trench containing the peptide nano-rings in the phase mode assisted visualizing the peptide nano-ring alignment more clearly. When the single trench was imaged with the height mode image in high-resolution (Fig. 3c), still only continuous packing of the nano-rings was observable as a line along the trench and the discrete Au nanoparticles could not resolve. But when the single trench was imaged in the phase mode in high-resolution, the discrete alignment of Au nanoparticles was observed, as shown in Fig. 3d. In this high-resolution image, the harder Au nanoparticles appeared to be brighter and the spacing between these nanoparticles was visible. The most of Au nanoparticles in Fig. 3d were self-assembled discretely without touching each other due to the spacing of the peptide nano-rings (Fig. 1). The darker nano-ring contrast around the Au nanoparticle, observed in the spin-coated sample in Fig. 2b, was not observed clearly in Fig. 3d, however this phase contrast difference between the spin-coated nano-rings and the self-assembled nano-rings may be caused by their topological difference. For the spin-coated sample the nano-rings were forced to pack closely by the external force on very smooth and flat TEM grids, and the resulting nano-ring monolayer also became relatively flat. Therefore, the detailed structure of nano-rings and Au nanoparticles was resolved in the AFM image of the spin-coated nano-ring sample due to the flatness of the coating. However, for the self-assembled sample, the nano-rings were self-assembled on rough surfaces consisting of alkyl SAMS and dithiol SAMs in different heights. The trenches were also not flat because the AFM cantilever could not shave alkyl SAMs smoothly and it further scraped the Au substrate partially. Shaved SAMs and Au substrate were piled at the edges of trenches, which also increased the roughness of the substrate. Since all different heights of SAMs, trenches, and edges contributed unevenness of the surface topology, the AFM resolution in the phase image on this self-assembled sample was degraded due to its surface roughness and it prevented to map the locations of the nano-rings and Au nanoparticles in the phase image. When the neat Au nanoparticles without the peptide nano-rings were assembled on the same dithiol-functionalized trenches, those Au nanoparticles were aligned as continuous lines without spacing in their phase AFM image. This observation supports that the Au nanoparticles observed in Fig. 3d were separated by the peptide nano-rings otherwise the spacing between Au nanoparticles should not be imaged. It should be noted that some of these nanoparticles seem to contact each other in Fig. 3d due to the deformation of the nano-rings during the self-assembly, which was also observed in the spin-coated sample in Fig. 2.

CONCLUSION

The peptide nano-rings containing Au nanoparticles inside their cavities were aligned on dithiol SAMs patterned as an array by AFM-based nanolithography. The peptide nano-rings were self-assembled as lines on these SAMs, and Au nanoparticles inside the nano-rings also formed lines with the spacing between these nanoparticles as the peptide nano-rings functioned as spacers. This type of fabrication will provide improved tunability in their optical properties of resulting nanoparticle-assembled arrays. In addition, optimization of the inter-particle distance of nanoparticles in the array with various spacers may allow one to design new types of photonics with desired optical properties. However, for those optical applications, the stability and the rigidity of the nano-rings will be more desirable to be improved since some of the nano-rings were deformed during the self-assembly and this deformation caused the uneven spacing of the nanoparticles on the array. For realistic photonic applications, the nanoparticle assembly needs to be accomplished without deformation because they require the perfect alignment of nanoparticles with minimum defects. The additions of hydrogen-bonding functional groups or polymerizing groups to the monomer may increase the rigidity of the nano-rings, which may help overcome this problem.

EXPERIMENTAL

Materials

Bis(*N*-α-amido-glycylglycine)-1,7-heptane dicarboxylate was synthesized and recrystallized in our lab by the published manner [36,37]. 1-Ethyl-3-[3-(dimethylamino)propyl]carbodiimide hydrochloride (EDAC), *N*-hydroxysuccinimide(NHS), 2-mercaptoethylamine, trimethylphosphinegold chloride, 16-mercaptohexadecanoic acid and octadecanothiol from Aldrich. Annealed gold substrates from Molecular Imaging. A series of trenches (100 nm × 1 μm) were made by shaving the alkylthiol SAM with a Si3N4

tip (Veeco Metrology) of the AFM (Nanoscope IIIa and MultiMode microscope, Digital Instruments). These trenches were made by customized Nanoscript software (VeecoMetrology). Formvar Film 200 Mesh Cu TEM grids were obtained from Electron Microscopy Sciences. UV-Lamp (14 mW/cm^2, 254 nm).

Preparation of Peptide Nano-rings

After peptide monomer of bis(*N*-α-amido-glycyl-glycine)-1,7-heptane dicarboxylate, 0.028 g, was dissolved in 10 mL of water and the pH of this solution was adjusted to 5.5 with citric acid, an excess amount of an organic Au precursor, trimethylphosphinegold chloride ($AuPMe_3Cl$) was added to this solution. After 5 days in the dark, the peptide nano-rings were observed in an outer diameter of 50 nm and an inner diameter of 15 nm. The nano-ring solution was washed with deionized water and centrifuged at 14.5 krpm, and then Au ions trapped inside the peptide nano-rings were reduced by a UV light (14 mW/cm^2, 254 nm) for 20 min. The resulting Au nanoparticles were observed to be about 15 nm in an average diameter from AFM images.

Nanolithography on Au Substrates

In order to pattern the peptide nano-rings containing Au nanoparticles in their cavities as an array on Au substrates, an array of dithiolated SAMs was patterned by a cantilever of an atomic force microscope (AFM) with the following sequence. First, 1-octadecanethiol (0.01 mM) was self-assembled on Au substrates in 99% ethanol at room temperature for 12 h. Then, an array of trenches (100 nm × 1 μm) was created by removing the alkylthiol SAMs by the tip of AFM via nanolithography technique [38–40]. On these trenches where Au surfaces were exposed, 16-mercaptohexadecanoic acid (0.01 mM) was self-assembled for overnight. After the resulting substrates were washed by deionized water, the end groups of the SAMs on trenches were functionalized by thiol via substituting carboxylic acid groups with thiol groups as shown in Scheme 1. In Scheme 1, 400 μL of ethyl-3-[3-(dimethylamino)propyl]carbodiimide (EDAC, 75 mM) and 400 μL of *N*-hydroxy succinimide (NHS, 15 mM) were immersed in aqueous solution containing the functionalized Au substrates for 30 min. Then, as shown in the step 3 in Scheme 1, 800 μL of 2-mercaptoethylamine (15 mM,) was incubated in the solution for 24 hrs to modify the ends groups of the SAMs in trenches to thiol groups [32,41].

Self-assembly of Au Nanoparticle-containing Peptide Nano-rings on Surfaces

When the peptide nano-rings containing Au nanoparticles in their cavities were mixed with the dithiolated SAM-patterned surfaces in aqueous solution for 8 hrs, the nano-rings were self-assembled on the trenches with the thiol-Au interaction. After these substrates were washed with deionized water, the attachment of the peptide nano-rings on the arrayed trenches was confirmed by AFM. While the height mode of AFM imaging was used to probe the topology of the nano-ring assembly, the phase mode of AFM imaging was applied to probe the location of Au nanoparticles since the distinguished hardness of surfaces between Au nanoparticles and peptide nano-rings allows us to image them respectively in the trenches.

We also assembled the peptide nano-rings containing Au nanoparticles on TEM grids by spin-coating to examine whether the nano-rings can be packed on surfaces without distraction. To obtain smooth surfaces of TEM grids, these grids were fixed on the top of mica substrates, which were also attached on AFM metal pucks. After the Au nanoparticle-containing peptide rings were spin-coated on the TEM grids, the resulting coatings were examined by AFM.

Acknowledgement

This work was supported by the US Department of Energy (DE-FG-02-01ER45935) and the National Science Foundation CARRER Award (ECS-0103430). Hunter College infrastructure is supported by the National Institutes of Health, the RCMI program (G12-RR-03037).

References

[1] Murray, C. B.; Kagan, C. R.; Bawendi, M. G. *Annu. Rev. Mater.* **2000**, *30*, 545.
[2] Yablonovitch, E. *Phys. Rev. Lett.* **1987**, *58*, 2059.
[3] Joannopoulos, J. D.; Villeneuve, P. R.; Fan, S. H. *Nature* **1997**, *387*, 830.
[4] Vlasov, Y. A.; Bo, X. Z.; Sturm, J. C.; Norris, D. *J. Nature* **2001**, *414*, 289–-293.
[5] Murray, C. B.; Kagan, C. R.; Bawendi, M. G. *Science* **1995**, *270*, 1335.
[6] Colvin, V. L. *MRS Bull.* **2001**, *26*, 637.
[7] Blanco, A.; Chomski, E.; Grabtchak, S.; Ibisate, M.; John, S.; Leonard, S. W.; Lopez, C.; Meseguer, F.; Miguez, H.; Mondia, J. P.; Ozin, G. A.; Toader, O.; van Driel, H. M. *Nature* **2000**, *405*, 437.
[8] Lin, S. Y.; Fleming, J. G.; Hetherington, D. L.; Smith, B. K.; Biswas, R.; Ho, K. M.; Sigalas, M. M.; Zubrzycki, W.; Kurtz, S. R.; Bur, *J. Nature* **1998**, *394*, 251.
[9] Liu, X.; Fu, L.; Hong, S.; Dravid, V. P.; Mirkin, C. A. *Adv. Mater.* **2002**, *14*, 231.
[10] Redl, F. X.; Cho, K. S.; Murray, C. B.; O'Brien, S. *Nature* **2003**, *423*, 968.
[11] Lee, W.; Chan, A.; Bevan, M. A.; Lewis, J. A.; Braun, P. V. *Langmuir* **2004**, *20*, 5262.
[12] Huang, J.; Kim, F.; Tao, A. R.; Connor, S.; Yang, P. *Nature Mater.* **2005**, *4*, 896.

[13] Kisailus, D.; Choi, J. H.; Weaver, J. C.; Yang, W. J.; Morse, D. E. *Adv. Mater.* **2005**, *17*, 314.
[14] Brott, L. L.; Naik, R. R.; Pikas, D. J.; Kirkpatrick, S. M.; Tomlin, D. W.; Whitlock, P. W.; Clarson, S. J.; Stone, M. O. *Nature* **2001**, *413*, 291.
[15] Whitling, J. M.; Spreitzer, G.; Wright, D. W. *Adv. Mater.* **2000**, *12*, 1377.
[16] Lee, S. Y.; Royston, E.; Culver, J. N.; Harris, M. T. *Nanotechnology* **2005**, *16*, S435.
[17] Douglas, T.; Young, M. *Adv. Mater.* **1999**, *11*, 679.
[18] Chatterji, A.; Ochoa, W. F.; Ueno, T.; Lin, T. W.; Johnson, J. E. *Nano Lett.* **2005**, *5*, 597.
[19] Walsh, D.; Arcelli, L.; Ikoma, T.; Tanaka, J.; Mann, S. *Nature Mater.* **2003**, *2*, 386.
[20] Sano, K. I.; Sasaki, H.; Shiba, K. *Langmuir* **2005**, *21*, 3090.
[21] Reches, M.; Gazit, E. *Science* **2003**, *300*, 625.
[22] Lee, S. W.; Mao, C. B.; Flynn, C. E.; Belcher, A. M. *Science* **2002**, *296*, 892.
[23] Gao, X.; Matsui, H. *Adv. Mater.* **2005**, *17*, 2037.
[24] Deng, Z. X.; Mao, C. D. *Nano Lett.* **2003**, *3*, 1545.
[25] Park, S. H.; Barish, R.; Li, H. Y.; Reif, J. H.; Finkelstein, G.; Yan, H.; LaBean, T. H. *Nano Lett.* **2005**, *5*, 693.
[26] Djalali, R.; Chen, Y.-F.; Matsui, H. *J. Am. Chem. Soc.* **2002**, *124*, 13660.
[27] Sarikaya, M.; Tamerler, C.; Jen, A. K. Y.; Schulten, K. *Nature Mater.* **2003**, *2*, 577.
[28] Naik, R. R.; Stringer, S. J.; Agarwal, G.; Jones, S. E.; Stone, M. O. *Nature Mater.* **2002**, *1*, 169.
[29] Yu, L.; Banerjee, I. A.; Matsui, H. *J. Am. Chem. Soc.* **2003**, *125*, 14837.
[30] Banerjee, I. A.; Yu, L.; Matsui, H. *Proc. Natl. Acad. Sci. USA* **2003**, *100*, 14678.
[31] Sumerel, J. L.; Yang, W. J.; Kisailus, D.; Weaver, J. C.; Choi, J. H.; Morse, D. E. *Chem. Mater.* **2003**, *15*, 4804.
[32] Banerjee, I. A.; Yu, L.; Matsui, H. *J. Am. Chem. Soc.* **2005**, *127*, 16002.
[33] Coffman, E. A.; Melechko, A. V.; Allison, D. P.; Simpson, M. L.; Doktycz, M. *J. Langmuir* **2004**, *20*, 8431.
[34] Djalali, R.; Jacopo, S.; Matsui, H. *J. Am. Chem. Soc.* **2004**, *126*, 7935.
[35] Djalali, R.; Chen, Y.-F.; Matsui, H. *J. Am. Chem. Soc.* **2003**, *125*, 5873.
[36] Kogiso, M.; Ohnishi, S.; Yase, K.; Masuda, M.; Shimizu, T. *Langmuir* **1998**, *14*, 4978.
[37] Matsui, H.; Gologan, B. *J. Phys. Chem. B.* **2000**, *104*, 3383.
[38] Liu, G. Y.; Xu, S.; Qian, Y. L. *Accounts Chem. Res.* **2000**, *33*, 457.
[39] Nuraje, N.; Banerjee, I. A.; MacCuspie, R. I.; Yu, L.; Matsui, H. *J. Am. Chem. Soc.* **2004**, *126*, 8088.
[40] Zhao, Z.; Banerjee, I. A.; Matsui, H. *J. Am. Chem. Soc.* **2005**, *127*, 8930.
[41] Frey, B. L.; Corn, R. M. *Anal. Chem.* **1996**, *68*, 3187.